

Shell-model coupled-cluster method for open-shell nuclei

Z. H. Sun,^{1,2} T. D. Morris,^{1,2} G. Hagen,^{2,1} G. R. Jansen,^{3,2} and T. Papenbrock^{1,2}

¹*Department of Physics and Astronomy, University of Tennessee, Knoxville, TN 37996, USA*

²*Physics Division, Oak Ridge National Laboratory, Oak Ridge, TN 37831, USA*

³*National Center for Computational Sciences, Oak Ridge National Laboratory, Oak Ridge, TN 37831, USA*

We present an approach to derive effective shell-model interactions from microscopic nuclear forces. The similarity-transformed coupled-cluster Hamiltonian decouples the single-reference state of a closed-shell nucleus and provides us with a core for the shell model. We use a second similarity transformation to decouple a shell-model space from the excluded space. We show that the three-body terms induced by both similarity transformations are crucial for an accurate computation of ground and excited states. As a proof of principle we use a nucleon-nucleon interaction from chiral effective field theory, employ a ^4He core, and compute low-lying states of ^{6-8}He and ^{6-8}Li in p -shell model spaces. Our results agree with benchmarks from full configuration interaction.

I. INTRODUCTION

Remarkable progress has been made in the ongoing endeavor to understand and predict nuclei from underlying nuclear forces. The computations of atomic nuclei, starting from Hamiltonians with nucleon-nucleon and three-nucleon forces are now starting to cover significant portions of the nuclear landscape, from light [1–3] to medium-mass [4–11], and to heavy nuclei [12, 13]. Theory now makes predictions for processes and observables that are hard to measure [14–17], and for nuclei that are hard to produce [13, 18]. This progress is due to realistic nuclear interactions [19–21] rooted in chiral effective field theory [22, 23], ideas from effective field theories and the renormalization group [24, 25] and application of methods which avoid the catastrophic scaling of full diagonalizations at the acceptable cost of approximations [26–33]. Here, we mention in particular the coupled-cluster (CC) [32, 34, 35] and the in-medium similarity renormalization group (IMSRG) [29, 33] methods, which perform a similarity transformation of the input Hamiltonian such that a product state is decoupled from particle-hole excitations (i.e., it becomes an exact eigenstate of the similarity transformed Hamiltonian).

In spite of all this progress, the description of open-shell nuclei still poses challenges. For decades the nuclear shell model [36–38] has been the method of choice to address open-shell nuclei accessible in one or two major oscillator shells. However, up until very recently, it has been a challenge to tie the applied effective shell-model interactions to the underlying nucleon-nucleon and three-nucleon interactions. The widely used microscopic derivation of effective interactions is usually based on many-body perturbation theory [39, 40], where certain diagrams are summed up to infinite order by using the folded-diagram method [41, 42]. However, the strong correlations of nuclear systems and the tensor property of the nuclear interactions spoil the order-by-order convergence of the effective interaction in this approach [43–45]. Alternative approaches to effective interactions contain both input from the underlying nucleon-nucleon interaction and phenomenological adjustments, which are

difficult to make for large shell-model spaces [46, 47]. The idea to derive the effective interaction from ab-initio methods [48, 49] has been fruitful: In this approach, one computes a doubly-magic nucleus with mass number A_c , and extracts the effective interaction from ab-initio calculations of nuclei with mass numbers $A = A_c + 1$ and $A = A_c + 2$ using Lee-Suzuki-Okamoto (LSO) techniques [50–53]. This idea was implemented using CC methods in Refs. [54, 55], respectively, starting from nucleon-nucleon and three-nucleon forces. However, some observables, such as charge radii, are sensitive to details of the high-lying excited states in the $A = A_c + 2$ system that are used in the construction of the effective interaction using the LSO projection technique.

The valence-space IMSRG (VS-IMSRG) [9, 56, 57] is an alternative that avoids this problem. In this approach, a non-perturbative effective interaction is derived within the IMSRG formalism [29], i.e., by decoupling a core and a valence space via similarity transformations. This avoids the problem of projecting high-lying states onto the valence space using the LSO technique, and, furthermore, the similarity transformation can be consistently applied to observables other than the energy, potentially offering insights into the origin of effective charges and the role of two-body currents. The similarity transformation induces many-body terms, and, at present, the VS-IMSRG and the IMSRG methods keep up to normal-ordered two-body operators. The effect of this truncation is currently not well understood.

In this paper, we want to follow the VS-IMSRG idea and generate effective interactions and operators via a decoupling of the core from the valence space. However, we base this decoupling, named shell-model coupled cluster (SMCC), on the CC approach. Like the VS-IMSRG, the SMCC is an extension of the closed-shell CC theory. After decoupling a closed-shell core with the CC method, we implement a second similarity transformation of the Hamiltonian, which decouples the valence space and the excluded space. In contrast to the VS-IMSRG, we perform this decoupling in a non-Hermitian way. This simplifies the working equations that implement the transformation. In this simplified set of working equations we

also explore the effect of three-body terms in the similarity transformation. We find that when the leading order three-body terms are included in the calculation of open p -shell nuclei, we obtain a much better agreement with exact results than what is achieved with the SMCC or VS-IMSRG methods truncated at the two-body level.

II. SHELL-MODEL COUPLED-CLUSTER METHOD

A. Single reference coupled-cluster

We start from the intrinsic Hamiltonian

$$H = \left(1 - \frac{1}{A}\right) \sum_{i=1}^A \frac{p_i^2}{2m} + \left(\sum_{i<j=1}^A v_{ij} - \frac{\vec{p}_i \cdot \vec{p}_j}{mA} \right). \quad (1)$$

Here A is the number of nucleons and v_{ij} is nucleon-nucleon potential. We note that if we are targeting an open system, then A may be larger than the A_c , the number of core-nucleons addressed in closed-shell CC theory.

We normal order the Hamiltonian H with respect to the Hartree-Fock state

$$|\Phi_0\rangle \equiv \prod_{i=1}^{A_c} a_i^\dagger |0\rangle \quad (2)$$

and obtain

$$\mathcal{H} = H - E_{\text{ref}} = \sum_{pq} f_{pq} \{p^\dagger q\} + \frac{1}{4} \sum_{pqrs} V_{pqrs} \{p^\dagger q^\dagger sr\}. \quad (3)$$

Here, the brackets $\{\dots\}$ indicate normal ordering, E_{ref} is the HF energy, f is the one-body interaction (also known as the Fock-matrix), V is the anti-symmetric two-body interaction, and p, q, r, s label single-particle states, see, e.g., Ref. [58] for details. In single-reference CC theory [32, 34, 35], the ground-state state is given by the exponential ansatz,

$$|\Psi_0\rangle = \exp(T)|\Phi_0\rangle. \quad (4)$$

Many-body correlations are introduced via the cluster operator

$$T = T_1 + T_2 + T_3 + \dots + T_{A_c}. \quad (5)$$

Here the cluster operators T_n create n -particle- n -hole excitations

$$T_n = \left(\frac{1}{n!}\right)^2 \sum_{\substack{a_1 a_2 \dots a_n \\ i_1 i_2 \dots i_n}} t_{i_1 i_2 \dots i_n}^{a_1 a_2 \dots a_n} \{a_1^\dagger a_2^\dagger \dots a_n^\dagger i_n i_{n-1} \dots i_1\}, \quad (6)$$

and $t_{i_1 i_2 \dots i_n}^{a_1 a_2 \dots a_n}$ are the corresponding amplitudes that need to be determined. The CC method yields the similarity-

transformed normal-ordered Hamiltonian

$$\begin{aligned} \overline{\mathcal{H}} &\equiv \exp(-T)\mathcal{H}\exp(T) \\ &= (\mathcal{H}\exp(T))_C \\ &= \Delta E + \sum_{pq} \overline{\mathcal{H}}_{pq} \{p^\dagger q\} + \sum_{pqrs} \overline{\mathcal{H}}_{pqrs} \{p^\dagger q^\dagger sr\} \\ &\quad + \sum_{pqrstu} \overline{\mathcal{H}}_{pqrstu} \{p^\dagger q^\dagger r^\dagger uts\} + \dots \end{aligned} \quad (7)$$

Here, ΔE is the correlation energy, i.e., the correction to the HF energy, and $\overline{\mathcal{H}}_{pq}$, $\overline{\mathcal{H}}_{pqrs}$ and $\overline{\mathcal{H}}_{pqrstu}$ are the one-, two-, and three-body part of $\overline{\mathcal{H}}$, respectively. The subscript C in the second line of Eq. (7) indicates that only connected diagrams enter the expression. The CC correlation energy and the amplitudes in Eq. (6) are determined by solving the following equations,

$$\langle \Phi_0 | \overline{\mathcal{H}} | \Phi_0 \rangle = \Delta E, \quad (8)$$

$$\langle \Phi_i^a | \overline{\mathcal{H}} | \Phi_0 \rangle = 0, \quad (9)$$

$$\langle \Phi_{ij}^{ab} | \overline{\mathcal{H}} | \Phi_0 \rangle = 0, \quad (10)$$

$$\langle \Phi_{ijk}^{abc} | \overline{\mathcal{H}} | \Phi_0 \rangle = 0. \quad (11)$$

⋮

So far we have not introduced any approximations. However, in practical calculations we need to truncate the cluster operator T at some low-order rank. The most commonly used approximation is CC with singles and doubles excitations (CCSD). In the CCSD approximation only Eqs. (9)-(10) are solved to determine the amplitudes. In this work we go beyond the CCSD approximation and include the leading-order three-particle-three-hole excitations in Eq. (11). This approximation is termed CCSDT-1 [59] and gives a significant improvement in the description of the ground-state. For closed shell systems, CCSD and CCSDT-1 typically capture around 90% and 99% of the full correlation energy, respectively [35].

B. Open-shell coupled-cluster

We now turn to the derivation of an effective shell-model interaction in our SMCC approach. We identify a valence space outside a closed shell core, and then divide the Hilbert space of $\overline{\mathcal{H}}$ into two complementary spaces P and Q with

$$P + Q = I. \quad (12)$$

Here the operator P is a projector onto the core and valence space, and Q is the excluded space. We seek a second similarity transformation that decouples the P and Q spaces, i.e.,

$$\overline{\overline{\mathcal{H}}} \equiv \exp(-S)\overline{\mathcal{H}}\exp(S), \quad (13)$$

such that

$$Q\overline{\overline{\mathcal{H}}}P = 0 \quad (14)$$

with

$$S = QSP. \quad (15)$$

In the second similarity transformation given in Eq. (13), we only retain the one- and two-body parts of the initial CCSDT-1 similarity transformed Hamiltonian $\overline{\mathcal{H}}$. The transformation fulfilling Eqs. (13) and (14) yields a non-Hermitian effective interaction

$$H_{\text{eff}} = P\overline{\overline{\mathcal{H}}}P = P \exp(-S)\overline{\mathcal{H}} \exp(S)P. \quad (16)$$

In analogy to the cluster operator T of Eq. (5), the operator S links the excluded space (Q) and the model space (P) and in general contains up to A -body terms.

Fig. 1 shows the three topologies of S that are found up to the two-body level. We notice that if one starts from the bare Hamiltonian in Eq. (1), there would be additional terms with a cluster structure. These are not present in the core-decoupled CC Hamiltonian $\overline{\mathcal{H}}$. The diagrams in Fig. 1 correspond to the amplitudes S_{ab} , S_{abcd} and S_{abci} , where we used labels a, b, c, \dots for particle states, and i, j, k, \dots for hole states.

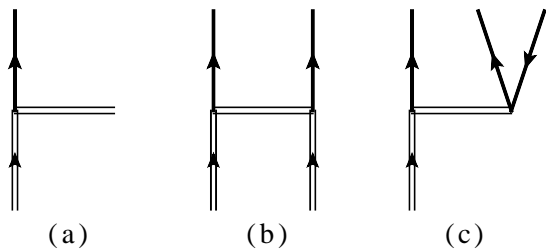


FIG. 1. Diagrams of the operator S that couple the valence space and the excluded space. The horizontal double bar is the S operator, with incoming and outgoing particle lines as indicated by arrows. The double incoming line denotes a particle inside the model space. Diagram (a) is a one-body operator, while diagrams (b) and (c) are two-body operators. The solid particle line is a general particle (i.e., either from the excluded space or the model space), except for the outgoing two particles in diagram (b), where at least one of the outgoing particles must be from the excluded space.

To determine the amplitudes of S proves to be less straightforward than doing so for the T amplitudes. Similar equations as those found in Eqs. (9)-(10) arise from Eq. (14),

$$\overline{\overline{\mathcal{H}}}_{ab} = 0, \quad (17)$$

$$\overline{\overline{\mathcal{H}}}_{abci} = 0, \quad (18)$$

$$\overline{\overline{\mathcal{H}}}_{abcd} = 0. \quad (19)$$

Inspired by the Magnus formulation of the IMSRG method [60], we adopt a constructive approach of building up S and solving Eqs. (17)-(19).

In the original formulation of the IMSRG, a unitary transformation which depends on a continuous variable t

is introduced, making a "flowing" transformed Hamiltonian,

$$H(t) = U^\dagger(t)HU(t). \quad (20)$$

The derivative of $H(t)$ with respect to t , denoted as $\dot{H}(t)$, yields

$$\dot{H}(t) = [\eta(t), H(t)] \quad (21)$$

$$\eta(t) = \dot{U}^\dagger(t)U(t). \quad (22)$$

Here η is chosen such that it eliminates the undesired matrix elements, and does so in a way that does not give rise to exceedingly stiff equations. With a suitable choice of η determined, Eq. (21) is solved until the undesired matrix elements are suppressed to an acceptable criteria. The Magnus formulation of the IMSRG dispenses with solving Eq. (21), and instead exploits the fact that Eq. (22) allows for a direct solution of the transformation $U(t)$ via the following expressions

$$U(t)^\dagger = \exp(\Omega(t)), \quad (23)$$

$$\dot{\Omega}(t) = \eta(t) - \frac{1}{2}[\Omega(t), \eta(t)] + \dots \quad (24)$$

There are several benefits to solving Eq. (24), most notably that observables can be solved one-by-one after a converged Ω is obtained. This is opposed to having to solve every desired observable other than the energy in parallel to the Hamiltonian, which would be prohibitively expensive for almost any single tensor operator except for a few scalar operators such as radii.

Taking inspiration from this Magnus formulation of the IMSRG, we solve an equation similar to Eq. (24) for our operator S ,

$$\dot{S}(t) = -\eta(\overline{\overline{\mathcal{H}}}(t)). \quad (25)$$

We have omitted all higher order terms in Eq. (24) because we only want to keep the form of S as it originates from Eqs. (17)-(19), and it is only important to find S that decouples the P and Q space, not what path is taken by the solver to arrive at the solution. We use the same definition of η as is used in the IMSRG except that our η is not anti-Hermitian. Its form will be discussed below. As η is a function of the Hamiltonian, one must generate the transformed Hamiltonian at each time step in order to decide which direction to take S . This is accomplished via the infinite Baker-Campbell-Hausdorff (BCH) expansion, and we truncate the expansion when nested commutators have matrix norms below a small threshold. Thus,

$$\begin{aligned} \overline{\overline{\mathcal{H}}} &= \overline{\mathcal{H}} + [\overline{\mathcal{H}}, S] + \frac{1}{2!} [[\overline{\mathcal{H}}, S], S] + \dots \\ &= \sum_{k=0}^{\infty} \frac{1}{k!} \text{ad}_S^k(\overline{\mathcal{H}}). \end{aligned} \quad (26)$$

Here $\text{ad}_S^0(\overline{\mathcal{H}}) = \overline{\mathcal{H}}$ and $\text{ad}_S^k(\overline{\mathcal{H}}) = [\text{ad}_S^{k-1}(\overline{\mathcal{H}}), S]$. Starting from two- and three-body Hamiltonians, the nested

commutators generate operators of increasing rank, and we need to introduce truncations. These will be discussed below.

There are several choices for the generator in Eq. (25) similar to the IMSRG [33], and in the current work we used the ‘‘White’’ generator [61]

$$\eta_{pqrs} = -\frac{\overline{\overline{\mathcal{H}}}_{pqrs}}{\overline{\overline{\mathcal{H}}}_{pp} + \overline{\overline{\mathcal{H}}}_{qq} - \overline{\overline{\mathcal{H}}}_{rr} - \overline{\overline{\mathcal{H}}}_{ss}}, \quad (27)$$

and the ‘‘Arc-tan White’’ generator

$$\eta_{pqrs} = -\frac{1}{2} \arctan \left(\frac{2\overline{\overline{\mathcal{H}}}_{pqrs}}{\overline{\overline{\mathcal{H}}}_{pp} + \overline{\overline{\mathcal{H}}}_{qq} - \overline{\overline{\mathcal{H}}}_{rr} - \overline{\overline{\mathcal{H}}}_{ss}} \right). \quad (28)$$

We first consider a truncation of Eq. (26) at the normal ordered two-body (NO2b) level, and refer to it as SMCC(2b). As we use nested commutators to evaluate the transformation leading to $\overline{\overline{\mathcal{H}}}$, we need only one general commutator expression for non-trivial contributions from two non-Hermitian operators χ and S . The one- and two-body contributions from the commutator are shown in Figs. 2 and 3, respectively. They lead to the following algebraic expressions for the one-body terms

$$\begin{aligned} [\chi, S]_{pq} &= \frac{1}{2} \sum_{abi} \chi_{piba} S_{baqi} \\ &+ \sum_{ia} \chi_{ia} S_{paqi} \\ &+ \sum_a (\chi_{pa} S_{aq} - S_{pa} \chi_{aq}), \end{aligned} \quad (29)$$

and the two-body terms

$$\begin{aligned} [\chi, S]_{pqrs} &= -\frac{1}{2} \sum_{ab} (\chi_{abrs} S_{pqab} - S_{abrs} \chi_{pqab}) \\ &- (1 - P_{pq})(1 - P_{rs}) \sum_{ia} \chi_{pias} S_{aqri} \\ &+ (1 - P_{pq}) \sum_a (\chi_{pa} S_{aqrs} - S_{pa} \chi_{aqrs}) \\ &- (1 - P_{rs}) \sum_a (\chi_{ar} S_{pqas} - S_{ar} \chi_{pqas}) \\ &- (1 - P_{rs}) \sum_i \chi_{ir} S_{pqis}. \end{aligned} \quad (30)$$

The matrix elements are antisymmetric through exchange of two equivalent external lines.

While truncating all intermediates at the NO2b level is expedient, the truncation comes at the cost of neglecting higher-body terms. It is instructive to look at the ground-state CC decoupling performed in this approximation. The similarity-transformed Hamiltonian can be written in two ways (as expressed in the following two lines)

$$\overline{\mathcal{H}} = \left[\mathcal{H} \left(1 + T + \frac{1}{2!} T^2 + \frac{1}{3!} T^3 + \frac{1}{4!} T^4 \right) \right]_C \quad (31)$$

$$= \mathcal{H} + [\mathcal{H}, T] + \frac{1}{2!} [[\mathcal{H}, T], T] + \dots \quad (32)$$

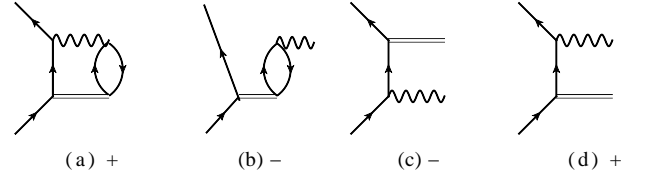


FIG. 2. Diagrammatic representation of $[\chi, S]^{1b}$ multiplied with a + or – sign from the commutator as indicated below each diagram. The wiggly line refers to the intermediate χ , and the horizontal double bar is S .

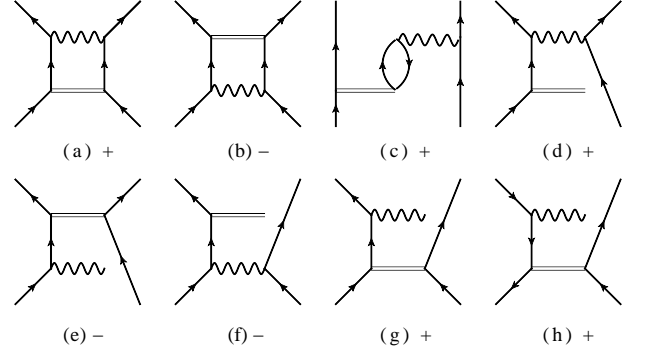


FIG. 3. Diagrammatic representation of $[\chi, S]^{2b}$ multiplied with a + or – sign from the commutator.

If we apply the NO2b approximation to each commutator in Eq. (32), we find some large omitted terms compared to Eq. (31). For example, a term contributing to $\frac{1}{2} \mathcal{H} T^2$ arises in equal parts from $[[\mathcal{H}, T_2]_{3b}, T_2]_{2b}$ and from $[[\mathcal{H}, T_2]_{1b}, T_2]_{2b}$. Here, the subscript $2b$ and $3b$ on the commutator denotes the truncation at the two- and three-body level, respectively, see Fig. 4. Thus using the NO2b truncation, one undercounts this class of terms by a factor of $\frac{1}{2}$. The IMSRG(2) approximation for ground-states also neglects such terms. These terms are repulsive, while perturbative triples are attractive. Thus, this undercounting explains why IMSRG(2) ground-state energies generally fall closer to the CCSD(T) approximation than to CCSD [33]. For this example it is clear that the effect of $[[\mathcal{H}, T_2]_{3b}, T_2]_{2b}$ can be restored simply in an ad-hoc fashion by double counting the half of these terms that arises from $[[\mathcal{H}, T_2]_{1b}, T_2]_{2b}$.

A similar situation appears in the open-shell decoupling. Fig. 5 shows a pair of ‘‘core polarization’’ diagrams in the open shell calculation that are neglected if the commutators are kept only at the two-body level. Cutting the diagrams as indicated at the red horizontal double bars clearly yields three-body terms. Numerical evaluations demonstrate that these diagrams, like their ground-state counterparts, make a substantial difference in the valence-space decoupling.

The inclusion of commutators with intermediate three-body terms is challenging because they should not affect the scaling of the storage required for our calculation. We proceed as follows. In each commutator evaluation,

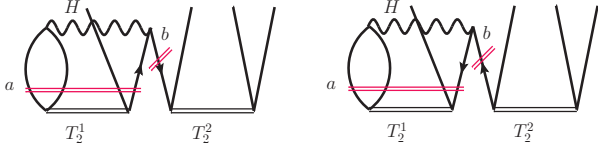


FIG. 4. (Color online) Two-body diagrams $[[\mathcal{H}, T_2], T_2]$ in CCSD closed-shell calculation. (Here, the black double horizontal bar denotes the cluster operator T , while the wiggly line is the Hamiltonian \mathcal{H} .) The intermediate 3-body $[[\mathcal{H}, T_2]_{3b}, T_2]_{2b}$ and one-body $[[\mathcal{H}, T_2]_{1b}, T_2]_{2b}$ terms inside the commutator result from making cuts at the locations a and b , respectively, and are indicated by red double lines.

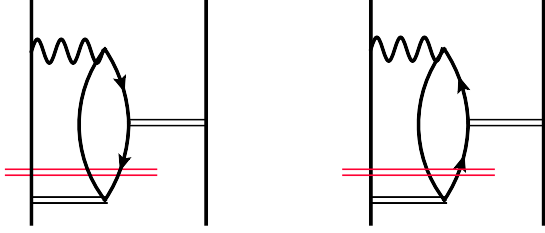


FIG. 5. (Color online) “Core polarization” diagrams that are neglected when all commutators are truncated at the two-body level. Cutting the diagrams at the red double bars reveals intermediate three-body terms.

the generated three-body diagrams are shown in Fig. 6.

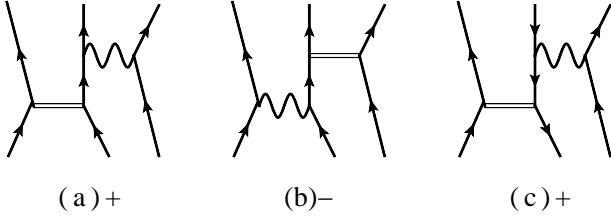


FIG. 6. Diagrammatic representation of $[\chi, S]_{3b}$ multiplied with a + or - sign from the commutator as indicated. Here χ and S are shown as wiggly and double horizontal lines, respectively.

They have the algebraic form

$$\begin{aligned} \chi_{pqrst} &= \mathcal{A} \sum_a (\bar{\mathcal{H}}_{qrau} S_{past} - S_{qrau} \bar{\mathcal{H}}_{past}) \\ &+ \sum_i \bar{\mathcal{H}}_{ipts} S_{rqui}, \end{aligned} \quad (33)$$

and the anti-symmetrizer is

$$\mathcal{A} \equiv (1 - P_{pq} - P_{pr})(1 - P_{us} - P_{ut}). \quad (34)$$

While seeking the solution of Eq. (14), we use the above expressions to keep all intermediate terms of the form $[[\bar{\mathcal{H}}_{2b}, S_{2b}]_{3b}, S_{2b}]_{2b}$. These terms are calculated on the fly without changing the scaling, since all of them can be factored into effective two-body pieces. Fig. 7 shows

the diagrams corresponding to these three-body terms we need to keep. Their algebraic form are found in Eq. (35). This approximation is labeled by SMCC(3b-diag), as it effectively keeps diagonal contributions from the three-body terms.

$$\begin{aligned} [[\chi, S]_{3b}, S]_{pqr} &= \frac{1}{2}(1 - P_{pq})(1 - P_{rs}) \sum_{abci} S_{bari} S_{pcb} \chi_{iqcs} \\ &+ (1 - P_{pq})(1 - P_{rs}) \sum_{abci} S_{basi} S_{pcrb} \chi_{qica} \\ &- (1 - P_{rs}) \sum_{abij} S_{bari} S_{pqbj} \chi_{ijas} \\ &- \frac{1}{2}(1 - P_{rs}) \sum_{abij} S_{basi} S_{pqrj} \chi_{jiba} \\ &- (1 - P_{rs}) \sum_{abci} S_{abir} \chi_{icas} S_{pqbc} \\ &- \frac{1}{2}(1 - P_{rs}) \sum_{abci} S_{basi} \chi_{ciba} S_{pqrc}. \end{aligned}$$

Contributions from $[[\bar{\mathcal{H}}_{2b}, S_{2b}]_{3b}, S_{2b}]_{2b}$ are neglected as they are too expensive to solve at each time step, and assumed to be of higher order.

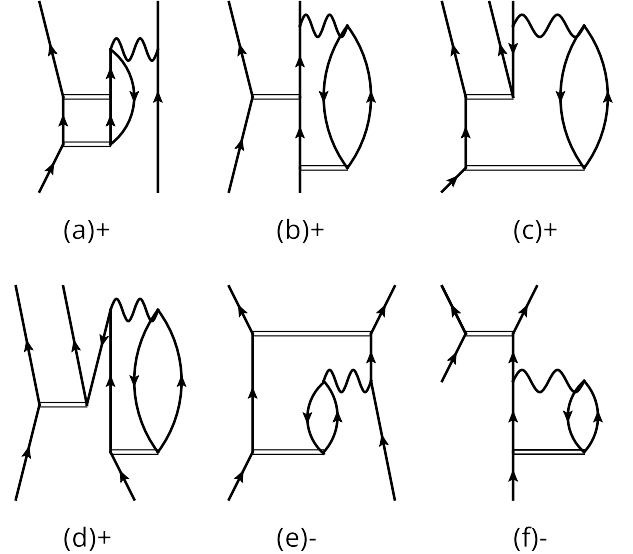


FIG. 7. Diagrams of $[[\chi_{2b}, S_{2b}]_{3b}, S_{2b}]_{2b}$ multiplied with a + or - sign from the commutator as indicated below each diagram. Here χ and S are shown as wiggly and double horizontal lines, respectively.

Our tests below show that shell-model interactions produced at the SMCC(3b-diag) approximation are still not satisfactory when compared to exact diagonalizations. We recall that an improved accuracy for the ground-state decoupling in CC theory requires us to include the leading order T_3 that is linear in T_2 . In the same spirit, we can generate the leading order part of S_3 by performing a third similarity transformation, where we keep only terms linear in S_2 that contribute to S_3 . The inclusion

of an approximation for S_3 is necessary, because there are three-body pieces of $\overline{\mathcal{H}}$ that violate the decoupling condition (14). If we keep only those parts linear in S_{2b} , then the elements of S_{3b} can be found as the approximate solutions of the following equations,

$$Q \exp(-S_{3b}) \overline{\mathcal{H}} \exp(S_{3b}) P \approx 0, \quad (35)$$

$$\left\{ [\overline{\mathcal{H}}_{2b}, S_{2b}] + [\overline{\mathcal{H}}_{1b}, S_{3b}] \right\}_{abcdij} = 0, \quad (36)$$

$$\left\{ [\overline{\mathcal{H}}_{2b}, S_{2b}] + [\overline{\mathcal{H}}_{1b}, S_{3b}] \right\}_{abcdei} = 0, \quad (37)$$

$$\left\{ [\overline{\mathcal{H}}_{2b}, S_{2b}] + [\overline{\mathcal{H}}_{1b}, S_{3b}] \right\}_{abcdef} = 0. \quad (38)$$

If we further approximate $\overline{\mathcal{H}}_{1b}$ above as containing only the diagonal one-body energies, then each of the three three-body topologies can be solved for generally as

$$S_{pqrst} = - \frac{[\overline{\mathcal{H}}_{2b}, S_{2b}]_{pqrst}}{\overline{\mathcal{H}}_{pp} + \overline{\mathcal{H}}_{qq} + \overline{\mathcal{H}}_{rr} - \overline{\mathcal{H}}_{ss} - \overline{\mathcal{H}}_{tt} - \overline{\mathcal{H}}_{uu}}. \quad (39)$$

Our goal is to generate an effective shell-model interaction, and we wish to study how contributions from S_3 will affect this interaction. For this purpose we generate the one- and two-body contributions of $\Delta \overline{\mathcal{H}} = P[\overline{\mathcal{H}}, S_{3b}]P$, and add them to the final valence interaction, and we refer to this as SMCC(3b-od), because it keeps ‘‘three-body off-diagonal’’ terms. We perform this operation once after converged S_{1b}, S_{2b} are obtained. This is akin to a perturbative treatment. If we were instead to solve the above equations iteratively, it would be akin to the CCSDT-1 process for decoupling the ground-state in CC theory. The elements we keep from $\Delta \overline{\mathcal{H}}$ can be organized into $[\overline{\mathcal{H}}_{2b}, S_{3b}]_{2b}$ and $[\overline{\mathcal{H}}_{2b}, S_{3b}]_{1b}$, and the corresponding diagrams are shown in Figs. 8 and 9, respectively. In each diagram, the short-wavelength small-amplitude wiggly line represents $\overline{\mathcal{H}}$, while the remaining diagram represents the three-body term (39) that is made from combining the three-body contraction $[\overline{\mathcal{H}}_{2b}, S_{2b}]_{3b}$ with the energy denominator.

In addition to the perturbative treatment of S_{3b} , we also keep the leading order three-body valence interaction of $\overline{\mathcal{H}}_{3b} \approx [\overline{\mathcal{H}}, S_{2b}]_{3b}$. This is important as the three-body valence interaction that we include would appear at second-order in the interaction. This procedure leads to a one-, two-, and three-body valence-space interaction, and we refer to this as the SMCC(3b) approximation.

C. Expectation values of observables in SMCC

As the similarity transformed Hamiltonian is not Hermitian when computed with the CC method, the evaluation of ground-state expectation values of operators other than the energy requires one to compute the left ground-state. This approach is based on response functions [62].

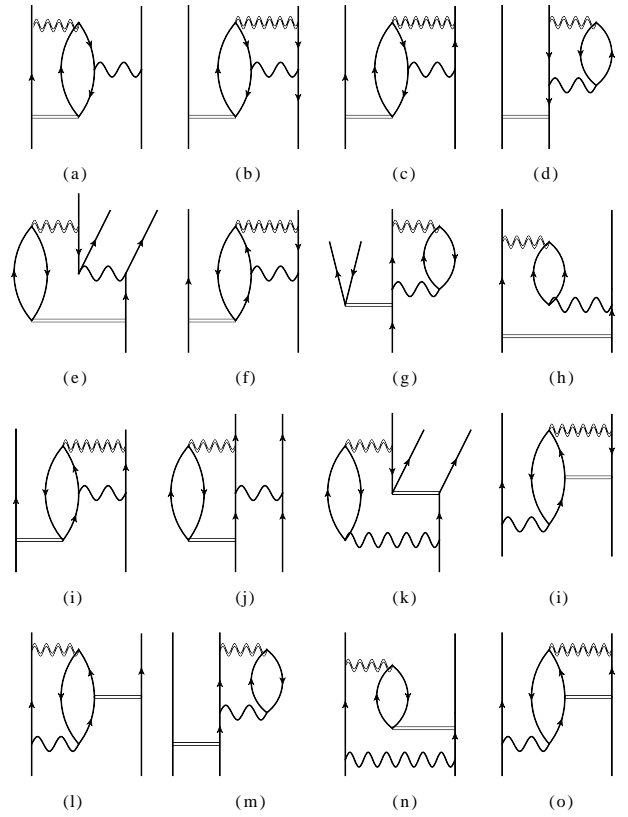


FIG. 8. Diagram representation of $[\overline{\mathcal{H}}_{2b}, S_{3b}]_{2b}$.

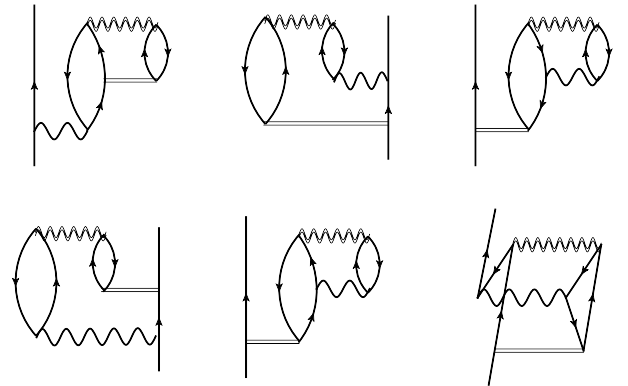


FIG. 9. Diagram representation of $[\overline{\mathcal{H}}_{2b}, S_{3b}]_{1b}$.

The left ground-state eigenvector is determined by

$$\langle \Phi_0 | (1 + \Lambda) (\overline{\mathcal{H}} - \Delta E) = 0, \quad (40)$$

where Λ is a de-excitation operator. The expectation value of a ground-state observable is then

$$O_c = \langle \Phi_0 | (1 + \Lambda) \overline{\mathcal{O}} | \Phi_0 \rangle. \quad (41)$$

For our valence-space approach, right states have the exact form of

$$|R_\nu\rangle = |\Phi_0\rangle \otimes |\Psi_\nu\rangle. \quad (42)$$

Here $|\Psi_\nu\rangle$ is the wave function obtained from a shell-model diagonalization. For the left, the interplay between the core and valence space are neglected. However, the terms affecting observables should still be adequately captured by approximating the left eigenvector as

$$\langle L_\nu| = \langle \Phi_0|(1 + \Lambda)| \otimes \langle \tilde{\Psi}_\nu|, \quad (43)$$

where $\langle \tilde{\Psi}_\nu|$ is a wave function obtained from an left diagonalization of $P\overline{\overline{H}}P$. This approximate expression makes it possible to deal with the core and valence space separately, and the expectation value of observables are calculated as

$$\langle L_\nu|O|R_\nu\rangle = O_c + \langle \tilde{\Psi}_\nu|O_\nu|\Psi_\nu\rangle. \quad (44)$$

In what follows, we will use this expression to compute ground-state radii.

III. RESULTS AND BENCHMARKS

We present results for the p -shell nuclei $^{6,7,8}\text{He}$ and $^{6,7,8}\text{Li}$ from the SMCC(2b) and SMCC(3b), and compare them with exact results from the full configuration interaction (FCI) approach, and with other approaches based on CC theory and IMSRG. We use the chiral nucleon-nucleon N^3LO interaction from Entem and Machleidt [63]. The bare interaction employs a cutoff at $\Lambda = 500$ MeV and is softened via the free-space similarity renormalization group method to the cutoff 1.9 fm^{-1} [64]. We neglect any three-body forces in this initial study in order to focus on the effects of the many-body terms induced by the valence-space decoupling. The two-body matrix elements are calculated in the spherical harmonic oscillator basis with $\hbar\omega = 24$ MeV. The model space consist of five major oscillator shells with single-particle angular momenta up to and including $l_{\text{max}} = 2$. This space consists of 76 single particle states and allows us to perform proof-of-principle and benchmark calculations.

The FCI results are obtained from an exact diagonalization of the Hamiltonian matrix. The coupled-cluster approach to the $A = 6, 7, 8$ nuclei is as follows. The $A = 6$ nucleus ^6He is computed with the two-particle attached equation-of-motion (EOM) coupled-cluster method by attaching two neutrons to the ^4He core. That approach includes $2p-0h$ and $3p-1h$ configurations [65–67]. The ^8He nucleus exhibits a closed sub shell and can be computed directly with coupled-cluster theory. Its ^8Li isobar is obtained from a charge-exchange EOM approach [68]. The VS-IMSRG computations of the $A = 6, 7, 8$ proceed as presented in [57]: The ^4He core is decoupled in the IMSRG(2) approximation and then followed by a valence-space decoupling and valence-space diagonalization using NushellX [69].

Let us first study the effect of induced three-body terms in the ground-state decoupling of the ^4He core. We calculated the energy of the ^4He core used in a ^6He diagonalization, employing IMSRG(2), CCSD(2b) [where

	IMSRG(2)	CCSD(2b)	CCSD(3b-diag)	CCSD	CCSDT-1
E(MeV)	-24.573	-24.626	-23.912	-23.911	-24.261

TABLE I. Ground-state energy of the ^4He core in a ^6He from CCSD variants and IMSRG(2).

each nested commutator keeps only two-body terms in analogy to SMCC(2b)], CCSD(3b-diag) [where diagonal three-body terms are kept in the spirit of SMCC(3b-diag)], CCSD, and CCSDT-1. Table I shows the results. CCSD(2b) is about 700 keV overbound, and qualitatively similar to the IMSRG(2) result supporting our claim that it is an undercounting of terms in Fig. 4 that separates IMSRG(2) from CCSD. We see that keeping $[[H, T_2]_{3b}, T]_{2b}$ in the CCSD(3b-diag) approximation almost matches full CCSD. This also suggests that our evaluation of the BCH expansion using nested commutators is appropriate. Calculations performed at the SMCC(3b) level yield similar results to CCSDT-1.

For the open-shell calculation of ^6He , we start from the one- and two-body CCSDT-1 Hamiltonian. This Hamiltonian has the ^4He core decoupled at the CCSDT-1 approximation; the induced three-body terms from CC are neglected. The p -shell effective interaction is obtained by decoupling the Hamiltonian with the SMCC method in the approximations discussed in the previous Section. The resulting shell-model interaction is used to calculate ^6He , and we compare those results with FCI. In the p -shell, ^6He is a two valence-neutron system with configurations $|(0p\frac{1}{2})^2\rangle^{0+}$, $|(0p\frac{3}{2})^2\rangle^{0+,2+}$ and $|(0p\frac{1}{2}0p\frac{3}{2})\rangle^{1+,2+}$. The occupations of the FCI wave functions show that the 0_1^+ and 2_1^+ states are dominated by p -shell components. For the 0_2^+ state, the ^4He core is broken and particles occupy the sd and pf shells. Similarly, the 2_2^+ and 1_1^+ states exhibit strong core polarization and sd components. The effective interaction will reproduce best those states that have largest overlap with the model space. Thus, the effective interaction works well for the low-lying states whose wave function are dominated by p -shell components. Our results are shown in Fig. 10. The EOM-CC result is from Ref. [65]. In that approach, ^6He is computed as a two-particle attached system of ^4He , including $2p-0h$ and $3p-1h$ configurations. The resulting ^6He ground-state energy is underbound by about 0.3 MeV compared to FCI. The SMCC(2b) 0^+ ground state is about 150 keV over bound compared with FCI, and the gap between the 0^+ and 2^+ states is about 0.6 MeV too large. The correction of $[[\chi, S]_{3b}, S_{2b}]_{2b}$ that enters SMCC(3b-diag) is very small, and this is in contrast to the closed-shell calculation of ^4He . The SMCC(3b-od) calculation including both $[[\chi, S]_{3b}, S]_{2b}$ and perturbative S_{3b} almost reproduces the EOM-CC results. This demonstrates that in open-shell calculations the elimination of off-diagonal induced three-body terms is crucial both for the binding energy and the energy spectrum. The VS-IMSRG(2) results here are similarly overbound as SMCC(2b).

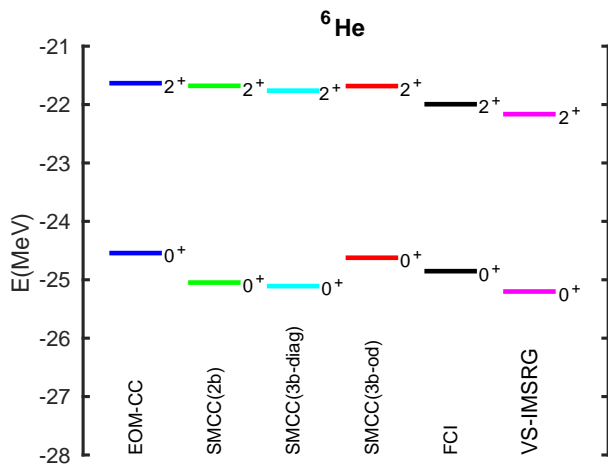


FIG. 10. (Color online) Spectrum of ${}^6\text{He}$ computed with various methods (FCI, EOM-CC and IMSRG) and compared to the SMCC results.

Fig. 11 compares the SMCC(3b-od) result of ${}^6\text{Li}$ with FCI and VS-IMSIRG. Here, both valence-space methods agree well with FCI.

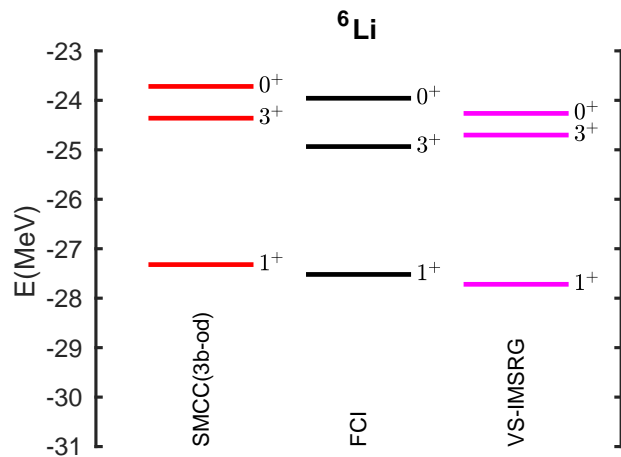


FIG. 11. (Color online) Spectrum of ${}^6\text{Li}$ computed with various methods (FCI and VS-IMSIRG) and compared to the SMCC(3b) result. SMCC(3b) include both three-body interaction diagonal and off-diagonal part.

The calculation of $A = 7$ nuclei is interesting as these have three valence nucleons. Fig. 12 shows the SMCC results for ${}^7\text{He}$ and compares them to FCI and VS-IMSIRG. The SMCC(3b-od) calculations both include $[[\chi, S]_{3b}, S]_{2b}$ and perturbative S_{3b} , while SMCC(3b) also employs valence three-body forces. Since the valence space now contains three nucleons, we can see whether the valence three-body force is important. For $A = 7$, nuclei, it yields a small amount of additional binding and causes the result to move toward better agreement

with FCI. The VS-IMSIRG again agrees roughly with the SMCC(2b) (not shown), and both poorly reproduce FCI.

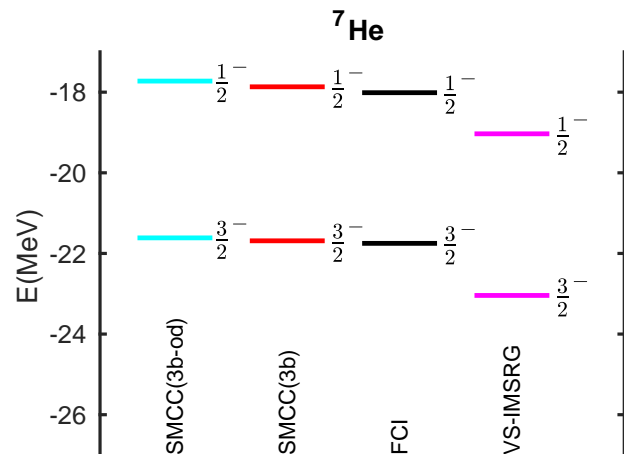


FIG. 12. (Color online) Spectrum of ${}^7\text{He}$ nucleus, computed with various methods (FCI, EOM-CC and VS-IMSIRG) and compared to the SMCC results.

For ${}^7\text{Li}$ the situation is similar to ${}^7\text{He}$, see Fig. 13), but the SMCC(3b-od) and SMCC(3b) are both under bound compared to FCI. We anticipate that an iterative treatment of the three-body forces in valence space would improve this result.

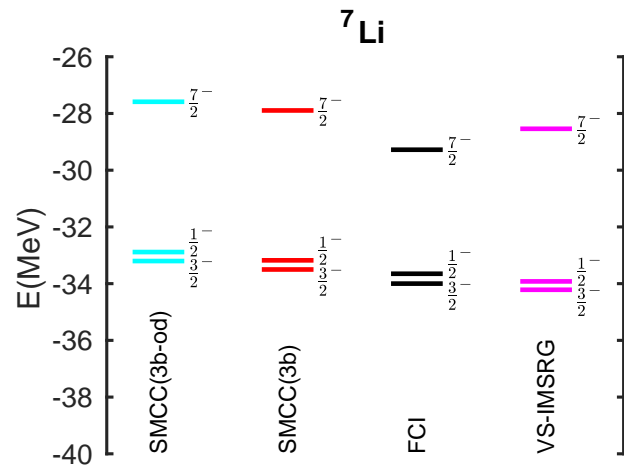


FIG. 13. (Color online) Same as Fig. 12 but for ${}^7\text{Li}$.

Finally, we turn to $A = 8$ nuclei. The closed sub-shell structure of ${}^8\text{He}$ makes it possible to compute this nucleus within single-reference CC method. Likewise, ${}^8\text{Li}$ can be calculated with charge-exchange EOM-CC [68] as a generalized excitation of ${}^8\text{He}$. Fig. 14 shows the comparison of the various methods in the calculation of ${}^8\text{He}$. The EOM-CC calculation is close to the FCI, while results from the recent CC effective interaction (CEI)

method [54, 55] underbinds ${}^8\text{He}$. The valence three-body force arising from SMCC(3b) makes it more bound on the order of 200 keV, and results in a good agreement with FCI. The VS-IMSRG results significantly overbinds, presumably because it also omits induced three-body effects.

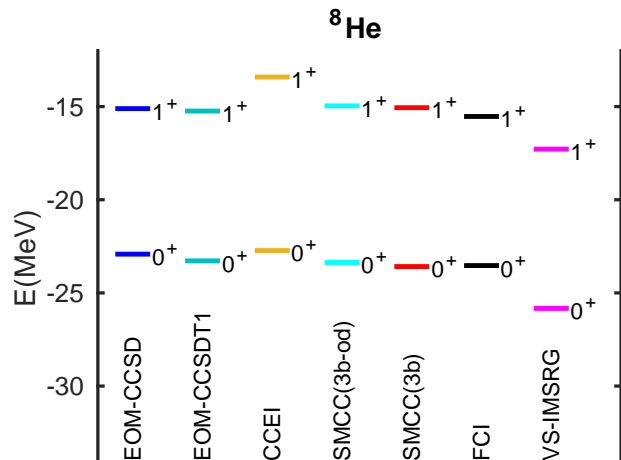


FIG. 14. (Color online) Spectrum of ${}^8\text{He}$ computed with various methods (FCI, EOM-CC, CCEI, and IMSRG) and compared to SMCC. The SMCC(3b-od) computation employs induced three-body forces that contribute to two-body forces, while SMCC(3b) also employs explicit three-body forces in the shell-model calculation.

Finally, we turn to ${}^8\text{Li}$ and show results in Fig. 15. The SMCC(3b) calculation is significantly improved by including the valence-space three-body force, on the order of 600 keV, and the low-lying states are in good agreement with FCI. The VS-IMSRG results reproduce spectra well, but overbind by about 2 MeV compared to FCI. The charge-exange calculation with EOM-CCSDT-1 reproduces the first three low-lying states well, while the higher-lying 0^+ probably lacks correlation energy from neglected higher order particle-hole excitations. Again, our results show that SMCC(3b) is an accurate tool for energy levels.

We also calculated the charge radii of He and Li isotopes with the approximate treatment of the left wave function. The core component is calculated in the CCSD approximation, which contains the zero-body part of the operator and the correction from the left (so called Λ) wavefunction. Fig. 16 shows the calculated charge radii from SMCC(3b) and VS-IMSRG and compares them to FCI results. We also calculated the charge radii using the Hellmann-Feynman method on top of the SMCC, though this approach is not correct because of the bi-variational structure of the CC energy functional. We note that the SMCC(3b) approach is closer to the FCI results than VS-IMSRG(2), but both methods are not as accurate as one would wish.

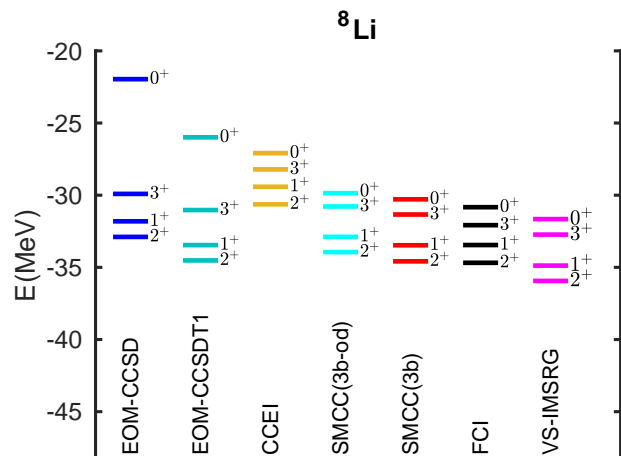


FIG. 15. (Color online) Same as Fig. 14 but for ${}^8\text{Li}$.

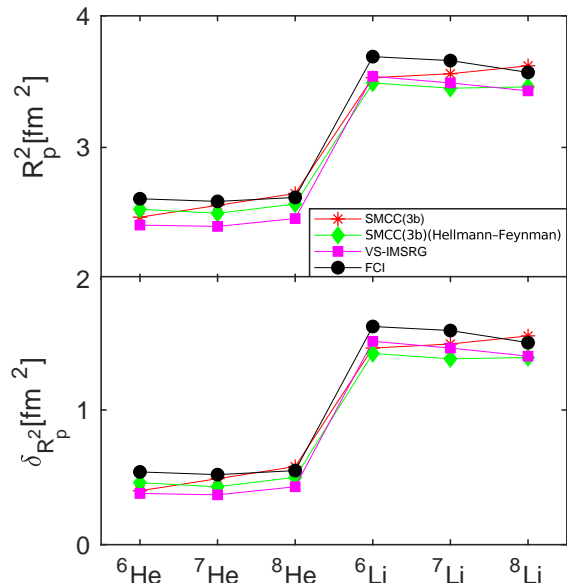


FIG. 16. (Color online) Squared point proton radii and isotope shift ($\delta R_p^2 = R_p^2 - R_p^2({}^4\text{He})$) of selected p -shell nuclei calculated using the SMCC(3b), the Hellmann-Feynman theorem [based on SMCC(3b)], the VS-IMSRG, and FCI.

IV. SUMMARY

We proposed a new non-perturbative microscopic method to derive effective interactions for the shell-model within the framework of coupled-cluster theory. The resulting shell-model coupled-cluster (SMCC) method is a promising route to perform precise calculations of open-shell nuclei with a large number of valence nucleons. Using renormalization group techniques, induced many-body forces generated by the similarity transformation

are included up to the three-body level. The effective interaction is applied to selected p -shell nuclei, and we obtained a good agreement with FCI results for energies and point-proton radii. We demonstrated that the inclusion of induced three-body forces is important for a precise computation of binding energies and spectra. The proposed method is a straightforward extension of the single reference coupled-cluster theory to the multi-reference system. It keeps the size-extensivity of the single reference coupled-cluster method, can be systematically improved, and is capable of dealing with more complex medium-mass nuclei.

ACKNOWLEDGMENTS

This material is based upon work supported by the U.S. Department of Energy, Office of Science, Office

of Nuclear Physics under Award Numbers DEFG02-96ER40963 (University of Tennessee), de-sc0008499 (SciDAC-3 NUCLEI), de-sc0018223 (SciDAC-4 NUCLEI), de-sc0015376 (Double-Beta Decay Topical Collaboration), and the Field Work Proposals ERKBP57 and ERKBP72 at Oak Ridge National Laboratory (ORNL). Computer time was provided by the Innovative and Novel Computational Impact on Theory and Experiment (INCITE) program. This research used resources of the Oak Ridge Leadership Computing Facility located at ORNL, which is supported by the Office of Science of the Department of Energy under Contract No. DE-AC05-00OR22725.

-
- [1] Steven C. Pieper and R. B. Wiringa, “Quantum Monte Carlo calculations of light nuclei,” *Ann. Rev. Nucl. Part. Sci.* **51**, 53–90 (2001).
- [2] Petr Navrátil, Sofia Quaglioni, Ionel Stetcu, and Bruce R. Barrett, “Recent developments in no-core shell-model calculations,” *Journal of Physics G: Nuclear and Particle Physics* **36**, 083101 (2009).
- [3] Bruce R. Barrett, Petr Navrátil, and James P. Vary, “Ab initio no core shell model,” *Prog. Part. Nucl. Phys.* **69**, 131 – 181 (2013).
- [4] Robert Roth, Sven Binder, Klaus Vobig, Angelo Calci, Joachim Langhammer, and Petr Navrátil, “Medium-Mass Nuclei with Normal-Ordered Chiral $NN+3N$ Interactions,” *Phys. Rev. Lett.* **109**, 052501 (2012).
- [5] G. Hagen, M. Hjorth-Jensen, G. R. Jansen, R. Machleidt, and T. Papenbrock, “Evolution of shell structure in neutron-rich calcium isotopes,” *Phys. Rev. Lett.* **109**, 032502 (2012).
- [6] V. Somà, A. Cipollone, C. Barbieri, P. Navrátil, and T. Duguet, “Chiral two- and three-nucleon forces along medium-mass isotope chains,” *Phys. Rev. C* **89**, 061301 (2014).
- [7] Timo A. Lähde, Evgeny Epelbaum, Hermann Krebs, Dean Lee, Ulf-G. Meißner, and Gautam Rupak, “Lattice effective field theory for medium-mass nuclei,” *Phys. Lett. B* **732**, 110 – 115 (2014).
- [8] H. Hergert, S. K. Bogner, T. D. Morris, S. Binder, A. Calci, J. Langhammer, and R. Roth, “Ab initio,” *Phys. Rev. C* **90**, 041302 (2014).
- [9] S. R. Stroberg, H. Hergert, J. D. Holt, S. K. Bogner, and A. Schwenk, “Ground and excited states of doubly open-shell nuclei from *ab initio* valence-space hamiltonians,” *Phys. Rev. C* **93**, 051301 (2016).
- [10] J. Simonis, S. R. Stroberg, K. Hebeler, J. D. Holt, and A. Schwenk, “Saturation with chiral interactions and consequences for finite nuclei,” *Phys. Rev. C* **96**, 014303 (2017).
- [11] E. Leistschneider, M. P. Reiter, S. Ayet San Andrés, B. Kootte, J. D. Holt, P. Navrátil, C. Babcock, C. Barbieri, B. R. Barquest, J. Bergmann, J. Bollig, T. Brunner, E. Dunling, A. Finlay, H. Geissel, L. Graham, F. Greiner, H. Hergert, C. Hornung, C. Jesch, R. Klawitter, Y. Lan, D. Lascar, K. G. Leach, W. Lippert, J. E. McKay, S. F. Paul, A. Schwenk, D. Short, J. Simonis, V. Somà, R. Steinbrügge, S. R. Stroberg, R. Thompson, M. E. Wieser, C. Will, M. Yavor, C. Andreoiu, T. Dickel, I. Dillmann, G. Gwinner, W. R. Plaß, C. Scheidenberger, A. A. Kwiatkowski, and J. Dilling, “Dawning of the $n = 32$ shell closure seen through precision mass measurements of neutron-rich titanium isotopes,” *Phys. Rev. Lett.* **120**, 062503 (2018).
- [12] Sven Binder, Joachim Langhammer, Angelo Calci, and Robert Roth, “Ab initio path to heavy nuclei,” *Phys. Lett. B* **736**, 119 – 123 (2014).
- [13] T. D. Morris, J. Simonis, S. R. Stroberg, C. Stumpf, G. Hagen, J. D. Holt, G. R. Jansen, T. Papenbrock, R. Roth, and A. Schwenk, “Structure of the lightest tin isotopes,” *Phys. Rev. Lett.* **120**, 152503 (2018).
- [14] Sofia Quaglioni and Petr Navrátil, “*Ab Initio* many-body calculations of $n-^3\text{H}$, $n-^4\text{He}$, $p-^3,^4\text{He}$, and $n-^{10}\text{Be}$ scattering,” *Phys. Rev. Lett.* **101**, 092501 (2008).
- [15] Evgeny Epelbaum, Hermann Krebs, Dean Lee, and Ulf-G. Meißner, “*Ab Initio* Calculation of the Hoyle State,” *Phys. Rev. Lett.* **106**, 192501 (2011).
- [16] S. Elhatisari, D. Lee, G. Rupak, E. Epelbaum, H. Krebs, T. A. Lähde, T. Luu, and U.-G. Meißner, “Ab initio alpha-alpha scattering,” *Nature* **528**, 111–114 (2015).
- [17] G. Hagen, A. Ekström, C. Forssén, G. R. Jansen, W. Nazarewicz, T. Papenbrock, K. A. Wendt, S. Bacca, N. Barnea, B. Carlsson, C. Drischler, K. Hebeler, M. Hjorth-Jensen, M. Miorelli, G. Orlandini, A. Schwenk, and J. Simonis, “Neutron and weak-charge distributions of the ^{48}Ca nucleus,” *Nature Physics* **12**, 186 (2016).
- [18] G. Hagen, G. R. Jansen, and T. Papenbrock, “Structure of ^{78}Ni from first-principles computations,” *Phys. Rev. Lett.* **117**, 172501 (2016).
- [19] K. Hebeler, S. K. Bogner, R. J. Furnstahl, A. Nogga, and A. Schwenk, “Improved nuclear matter cal-

- culations from chiral low-momentum interactions,” *Phys. Rev. C* **83**, 031301 (2011).
- [20] Robert Roth, Joachim Langhammer, Angelo Calci, Sven Binder, and Petr Navrátil, “Similarity-Transformed Chiral $NN + 3N$ Interactions for the *Ab Initio* Description of ^{12}C and ^{16}O ,” *Phys. Rev. Lett.* **107**, 072501 (2011).
- [21] A. Ekström, G. R. Jansen, K. A. Wendt, G. Hagen, T. Papenbrock, B. D. Carlsson, C. Forssén, M. Hjorth-Jensen, P. Navrátil, and W. Nazarewicz, “Accurate nuclear radii and binding energies from a chiral interaction,” *Phys. Rev. C* **91**, 051301 (2015).
- [22] E. Epelbaum, H.-W. Hammer, and Ulf-G. Meißner, “Modern theory of nuclear forces,” *Rev. Mod. Phys.* **81**, 1773–1825 (2009).
- [23] R. Machleidt and D.R. Entem, “Chiral effective field theory and nuclear forces,” *Physics Reports* **503**, 1 – 75 (2011).
- [24] S. K. Bogner, T. T. S. Kuo, and A. Schwenk, “Model-independent low momentum nucleon interaction from phase shift equivalence,” *Physics Reports* **386**, 1 – 27 (2003).
- [25] S.K. Bogner, R.J. Furnstahl, and A. Schwenk, “From low-momentum interactions to nuclear structure,” *Prog. Part. Nucl. Phys.* **65**, 94 – 147 (2010).
- [26] W.H. Dickhoff and C. Barbieri, “Self-consistent green’s function method for nuclei and nuclear matter,” *Prog. Part. Nucl. Phys.* **52**, 377 – 496 (2004).
- [27] S. Gandolfi, F. Pederiva, S. Fantoni, and K. E. Schmidt, “Auxiliary field diffusion monte carlo calculation of nuclei with $a \leq 40$ with tensor interactions,” *Phys. Rev. Lett.* **99**, 022507 (2007).
- [28] Dean Lee, “Lattice simulations for few- and many-body systems,” *Prog. Part. Nucl. Phys.* **63**, 117 – 154 (2009).
- [29] K. Tsukiyama, S. K. Bogner, and A. Schwenk, “In-Medium Similarity Renormalization Group For Nuclei,” *Phys. Rev. Lett.* **106**, 222502 (2011).
- [30] Sven Binder, Piotr Piecuch, Angelo Calci, Joachim Langhammer, Petr Navrátil, and Robert Roth, “Extension of coupled-cluster theory with a noniterative treatment of connected triply excited clusters to three-body hamiltonians,” *Phys. Rev. C* **88**, 054319 (2013).
- [31] V. Somà, C. Barbieri, and T. Duguet, “*Ab initio* gorkov-green’s function calculations of open-shell nuclei,” *Phys. Rev. C* **87**, 011303 (2013).
- [32] G. Hagen, T. Papenbrock, M. Hjorth-Jensen, and D. J. Dean, “Coupled-cluster computations of atomic nuclei,” *Rep. Prog. Phys.* **77**, 096302 (2014).
- [33] H. Hergert, S. K. Bogner, T. D. Morris, A. Schwenk, and K. Tsukiyama, “The in-medium similarity renormalization group: A novel *ab initio* method for nuclei,” *Phys. Rep.* **621**, 165 – 222 (2016).
- [34] H. Kümmel, K. H. Lührmann, and J. G. Zabolitzky, “Many-fermion theory in expS - (or coupled cluster) form,” *Physics Reports* **36**, 1 – 63 (1978).
- [35] Rodney J. Bartlett and Monika Musiał, “Coupled-cluster theory in quantum chemistry,” *Rev. Mod. Phys.* **79**, 291–352 (2007).
- [36] B. A. Brown and B. H. Wildenthal, “Status of the nuclear shell model,” *Ann. Rev. Nucl. Part. Sci.* **38**, 29–66 (1988).
- [37] E. Caurier, G. Martínez-Pinedo, F. Nowacki, A. Poves, and A. P. Zuker, “The shell model as a unified view of nuclear structure,” *Rev. Mod. Phys.* **77**, 427–488 (2005).
- [38] Noritaka Shimizu, Takashi Abe, Yusuke Tsunoda, Yutaka Utsuno, Tooru Yoshida, Takahiro Mizusaki, Michio Honma, and Takaharu Otsuka, “New-generation monte carlo shell model for the k computer era,” **2012**, 01A205 (2012).
- [39] Morten Hjorth-Jensen, Thomas T.S. Kuo, and Eivind Osnes, “Realistic effective interactions for nuclear systems,” *Physics Reports* **261**, 125 – 270 (1995).
- [40] L. Coraggio, A. Covello, A. Gargano, N. Itaco, and T. T. S. Kuo, “Shell-model calculations and realistic effective interactions,” *Prog. Part. Nucl. Phys.* **62**, 135 – 182 (2009).
- [41] T. T. S. Kuo, S. Y. Lee, and K. F. Ratcliff, “A folded-diagram expansion of the model-space effective hamiltonian,” *Nuclear Physics A* **176**, 65 – 88 (1971).
- [42] B. H. Brandow, “Linked-cluster expansions for the nuclear many-body problem,” *Rev. Mod. Phys.* **39**, 771–828 (1967).
- [43] Bruce R. Barrett and Michael W. Kirson, “Higher-order terms and the apparent non-convergence of the perturbation expansion for the effective interaction in finite nuclei,” *Nuclear Physics A* **148**, 145 – 180 (1970).
- [44] J. P. Vary, P. U. Sauer, and C. W. Wong, “Convergence rate of intermediate-state summations in the effective shell-model interaction,” *Phys. Rev. C* **7**, 1776–1785 (1973).
- [45] T. H. Schücan and H. A. Weidenmüller, “Perturbation theory for the effective interaction in nuclei,” *Annals of Physics* **76**, 483 – 509 (1973).
- [46] M. Honma, T. Otsuka, B. A. Brown, and T. Mizusaki, “Effective interaction for pf-shell nuclei,” *Phys. Rev. C* **65**, 061301 (2002).
- [47] B. Alex Brown and W. A. Richter, “New “usd” hamiltonians for the sd shell,” *Physical Review C (Nuclear Physics)* **74**, 034315 (2006).
- [48] A. F. Lisetskiy, B. R. Barrett, M. K. G. Kruse, P. Navratil, I. Stetcu, and J. P. Vary, “*Ab-initio* shell model with a core,” *Phys. Rev. C* **78**, 044302 (2008).
- [49] E. Dikmen, A. F. Lisetskiy, B. R. Barrett, P. Maris, A. M. Shirokov, and J. P. Vary, “*Ab initio* effective interactions for *sd*-shell valence nucleons,” *Phys. Rev. C* **91**, 064301 (2015).
- [50] K. Suzuki and S. Y. Lee, “Convergent theory for effective interaction in nuclei,” *Prog. Theo. Phys.* **64**, 2091 (1980).
- [51] K. Suzuki, “Construction of hermitian effective interaction in nuclei: general relation between hermitian and non-hermitian forms ,” *Prog. Theo. Phys.* **68**, 246–260 (1982).
- [52] Kenji Suzuki, “Reformulation of coupled-cluster theory for many-fermion system on similarity-transformation theory,” *Progress of Theoretical Physics* **87**, 937–955 (1992).
- [53] K. Suzuki, R. Okamoto, and H. Kumagai, “Many-body theory in terms of effective interactions and its relation to coupled-cluster method,” *Nucl. Phys. A* **580**, 213 – 235 (1994).
- [54] G. R. Jansen, J. Engel, G. Hagen, P. Navratil, and A. Signoracci, “*Ab Initio* coupled-cluster effective interactions for the shell model: Application to neutron-rich oxygen and carbon isotopes,” *Phys. Rev. Lett.* **113**, 142502 (2014).
- [55] G. R. Jansen, M. D. Schuster, A. Signoracci, G. Hagen, and P. Navrátil, “Open *sd*-shell nuclei from first princi-

- ples,” *Phys. Rev. C* **94**, 011301 (2016).
- [56] S. K. Bogner, H. Hergert, J. D. Holt, A. Schwenk, S. Binder, A. Calci, J. Langhammer, and R. Roth, “Nonperturbative shell-model interactions from the in-medium similarity renormalization group,” *Phys. Rev. Lett.* **113**, 142501 (2014).
- [57] S. R. Stroberg, A. Calci, H. Hergert, J. D. Holt, S. K. Bogner, R. Roth, and A. Schwenk, “Nucleus-dependent valence-space approach to nuclear structure,” *Phys. Rev. Lett.* **118**, 032502 (2017).
- [58] I. Shavitt and R. J. Bartlett, *Many-body Methods in Chemistry and Physics* (Cambridge University Press, Cambridge UK, 2009).
- [59] Yoon S. Lee, Stanislaw A. Kucharski, and Rodney J. Bartlett, “A coupled cluster approach with triple excitations,” *The Journal of Chemical Physics* **81**, 5906–5912 (1984).
- [60] T. D. Morris, N. M. Parzuchowski, and S. K. Bogner, “Magnus expansion and in-medium similarity renormalization group,” *Phys. Rev. C* **92**, 034331 (2015).
- [61] Steven R. White, “Numerical canonical transformation approach to quantum many-body problems,” *The Journal of Chemical Physics* **117**, 7472–7482 (2002).
- [62] E. A. Salter, Gary W. Trucks, and Rodney J. Bartlett, “Analytic energy derivatives in many-body methods. i. first derivatives,” *The Journal of Chemical Physics* **90**, 1752–1766 (1989).
- [63] D. R. Entem and R. Machleidt, “Accurate charge-dependent nucleon-nucleon potential at fourth order of chiral perturbation theory,” *Phys. Rev. C* **68**, 041001 (2003).
- [64] S. K. Bogner, R. J. Furnstahl, and R. J. Perry, “Similarity renormalization group for nucleon-nucleon interactions,” *Phys. Rev. C* **75**, 061001 (2007).
- [65] G. R. Jansen, M. Hjorth-Jensen, G. Hagen, and T. Papenbrock, “Toward open-shell nuclei with coupled-cluster theory,” *Phys. Rev. C* **83**, 054306 (2011).
- [66] G. R. Jansen, “Spherical coupled-cluster theory for open-shell nuclei,” *Phys. Rev. C* **88**, 024305 (2013).
- [67] J. R. Gour, M. Horoi, P. Piecuch, and B. A. Brown, “Coupled-Cluster and Configuration-Interaction Calculations for Odd-*A* Heavy Nuclei,” *Phys. Rev. Lett.* **101**, 052501 (2008).
- [68] A. Ekström, G. R. Jansen, K. A. Wendt, G. Hagen, T. Papenbrock, S. Bacca, B. Carlsson, and D. Gazit, “Effects of three-nucleon forces and two-body currents on gamow-teller strengths,” *Phys. Rev. Lett.* **113**, 262504 (2014).
- [69] B. A. Brown and W. D. M. Rae, “The shell-model code nushellx@msu,” *Nuclear Data Sheets* **120**, 115 – 118 (2014).